engineering proceedings

MDPI

Proceeding Paper

Valorization of a New Benzimidazole-Based Green Inhibitor: Theoretical DFT Studies †

Oualid Sokkah *, Hicham Essassaoui, Aziz Ihammi, Darifa Addichi, Saliha Loughmari, Mohamed Ellouz and Mohammed Chigr

Advanced Chemistry & Applied Organic Chemistry Laboratory (LCA&COA), Faculty of Sciences and Technology, Sultan Moulay Slimane University, P.O. Box 523, Beni-Mellal 23000, Morocco; hichambcg@gmail.com (H.E.); azizihammi@gmail.com (A.I.); darifaadd@gmail.com (D.A.); salihaloughmari@gmail.com (S.L.); ellouz.chimie@gmail.com (M.E.); chigrm@gmail.com (M.C.)

* Correspondence: oualid.sokkah@gmail.com

† Presented at the 2nd International Conference on Sciences and Techniques for Renewable Energy and the Environment, Al Hoceima, Morocco, 28–30 April 2026.

Abstract

Benzimidazole derivatives are widely used as a drug. In this work, we valorized the electrochemical activities of our new Benzimidazole-derived compound, 2-(4-chlorophenyl)-4-nitro-1H-benzimidazole (OS1), as a green inhibitor that can be used in environmental applications, which gives rise to a tautomeric equilibrium (A and B), applied to mild steel in a 1 M HCl solution. The inhibitory effect of 2-(4-chlorophenyl)-4-nitro-1H-benzimidazole (OS1) on carbon steel (CS) corrosion in 1 M HCl was evaluated with DFT studies. The value ΔN = 0.019 for A and 0.057 is positive and less than 3.6, indicating that the molecule functions as an electron donor towards the iron substrate, creating a shielding layer that prevents corrosion. DFT results identified the nucleophilic that C(4,6,24) N(12) O(15) and Cl(27) in A and C(4,5,6,32) O(14,15) and Cl(26) in B and electrophilic C(6) N(12) and O(15) in A and O(14,15) in B attack sites. Notably, these findings established that Tautomer A is the most stable.

Keywords: benzimidazole; density functional theory; 2-(4-chlorophenyl)-4-nitro-1H-benzo[d]imidazole; green inhibitor

1. Introduction

Corrosion inhibitors play a crucial role in industry by protecting metallic materials from degradation [1]. Even at low concentrations, these compounds can significantly reduce or slow down corrosion by forming a protective layer that separates the metal surface from its surrounding environment [2]. Their mode of interaction with the surface, whether through physisorption or chemisorption, depends largely on their chemical composition [3]. Although inorganic inhibitors are commonly used, organic inhibitors have gained prominence due to their high efficiency, as they create stable and protective molecular films on metal surfaces [4].

In this study, we prepared a novel series of benzimidazole derivatives that, in addition to their remarkable corrosion inhibition properties [5], exhibit a wide range of pharmacological activities [6]. Functionalized benzimidazole compounds, bearing diverse substituents, constitute key structural frameworks in many therapeutic agents [7], including drugs with anticancer and antiprotozoal effects, as well as antiviral activity. Moreover, these derivatives are widely recognized for their antibacterial [8], anti-inflammatory [9], antifungal,

Check for updates

Academic Editors: Charaf Laghlimi, Younes Ziat, Zakaryaa Zarhri, Noureddine Lakouari and Hamza BelkhanchiName

Published: 23 June 2026

Copyright: © 2026 by the authors. Licensee MDPI, Basel, Switzerland. This article is an open access article distributed under the terms and conditions of the Creative Commons Attribution (CC BY) license.

antihypertensive [10], and antituberculosis properties, and have also shown significant effectiveness in the treatment of HIV [9].

Our study began with the synthesis of a novel series of benzimidazole-based heterocycles by condensation of an aldehyde onto an ortho-phenylenediamine derivative. This research focuses on 2-(4-chlorophenyl)-4-nitro-1H-benzimidazole (OS1), which exists in a tautomeric equilibrium (Forms A and B) [11].

Before addressing this topic, it is first necessary to have a general overview of the inhibitory activity of our molecule, using the DFT study.

Following synthesis, the relative stability of these tautomers was determined via DFT calculations [5]. The inhibitory performance was then evaluated through an electrochemical study. To complement the experimental data, comprehensive theoretical analyses were performed.

Gas-phase DFT: It was conducted at the B3LYP/6-311++G(d,p) level using Gaussian 09W to evaluate thermodynamic functions and atomic Fukui indices [5].

2. Methods and Materials

2.1. Materials

The B3LYP exchange-correlation functional, in combination with the 6-311++G(d,p) basis set [5], was employed for all DFT computations. Frequency calculations were conducted to ensure the convergence of stationary points, while GaussView 6 was used to generate spin density isosurfaces.

2.2. Synthesis of the Inhibitor

Synthesis of OS1 (Foreseen)

3-Nitro-o-phenylenediamine (250 mg, 1.63 mmol) and 4-chlorobenzaldehyde (230 mg, 1.63 mmol) were dissolved in 20 mL of DMSO in a 50 mL round-bottom flask. After adding sodium metabisulfite (930 mg, 5 mmol) as an oxidant, the reaction was refluxed for 4–5 h (monitored by TLC). The mixture was then cooled, quenched with 30 mL of water, and the precipitate filtered (Figure 1).

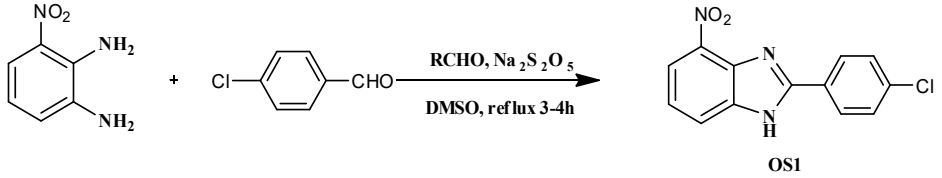


Figure 1. Formation of 2-(4-chlorophenyl)-4-nitro-1H-benzimidazole.

OS1 exists as an equilibrium between two tautomeric forms, A and B. To evaluate their relative thermodynamic stability, a theoretical study was conducted using density functional theory (DFT) calculations (Figure 2).

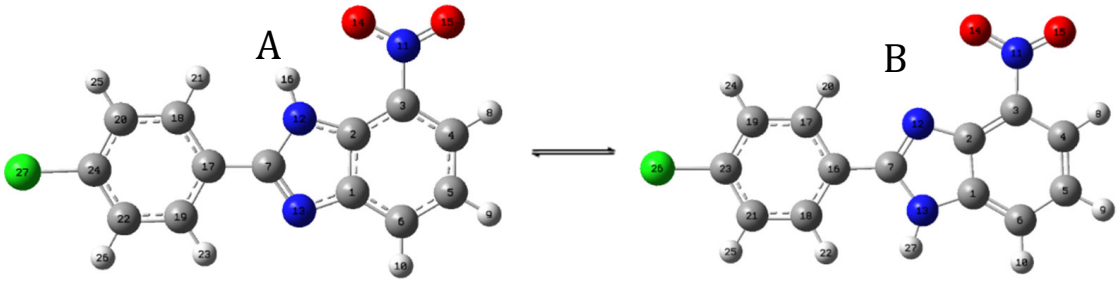


Figure 2. The two tautomeric forms (**A**,**B**), of 2-(4-chlorophenyl)-4-nitro-1H-benzimidazole (OS1).

https://doi.org/10.3390/engproc2026144005

2.3. DFT Study

Key reactivity indices and inhibitory efficiency descriptors were calculated based on the HOMO and LUMO energies. These frontier orbital parameters allow for a quantitative assessment of the interaction between the inhibitor molecules and the metal surface.

The electron-donating and electron-accepting abilities of the inhibitors are characterized by their E_{HOMO} and E_{LUMO} values, respectively. From these, the energy gap (ΔE_{gap}) is calculated. A reduced energy gap is associated with increased molecular reactivity and improved inhibitory performance, as noted in previous studies (1).

Electronegativity (χ) represents the power of a molecule to attract electrons [12] (2).

Chemical reactivity was further evaluated through global hardness (η), which quantifies the resistance toward electronic cloud deformation and charge transfer [5]. Effective inhibitors are generally characterized by low η values, indicating a soft polarizable nature that favors adsorption onto the iron electrode (3).

The fraction of transferred electrons (ΔN) was determined to estimate the electronic interaction between the inhibitor and the metal. This parameter was calculated using the theoretical electronegativity of iron ($\chi_{Fe} \approx 4.82$ eV) and its global hardness ($\eta_{Fe} = 0$ eV) [13]. According to the Lukovits equation, a ΔN value within the range of $0 < \Delta N < 3.6$ signifies that the inhibitor molecule effectively acts as an electron donor to the iron surface (4).

To identify the specific reactive sites within the inhibitor molecules, Hirshfeld charges were calculated for the neutral (N), cationic (N − 1), and anionic (N + 1) states using the NBO code [14]. These atomic charges were subsequently processed in Multiwfn to generate Fukui functions (f^+ and f^-) according to Equations (5) and (6). These indices allow for a precise mapping of nucleophilic and electrophilic centers across the molecular framework.

$$\Delta E_{GAP} = E_{LUMO} - E_{HOMO} \quad (1)$$

$$\chi = -\frac{(E_{LUMO} + E_{HOMO})}{2} \quad (2)$$

$$\eta = \frac{E_{LUMO} - E_{HOMO}}{2} \quad (3)$$

$$\Delta N = \frac{\chi_{Fe} - \chi_{inh}}{2(\eta_{Fe} + \eta_{inh})} \quad (4)$$

$$f_k^+ = q_k^N - q_k^{N+1} \text{ (for nucleophilic attack)} \quad (5)$$

$$f_k^- = q_k^{N-1} - q_k^N \text{ (for electrophilic attack)} \quad (6)$$

3. Results and Discussion

3.1. DFT Results

The electronic properties of the optimized structures were evaluated by calculating the E_{HOMO} and E_{LUMO} levels. The difference between these values, defined as the energy gap (ΔE_{gap}), was used to assess the reactivity and inhibitory potential of the OS1 tautomers (Figure 3). The green zone represents the positive phase and the red zone represents the negative phase of the orbital.

https://doi.org/10.3390/engproc2026144005

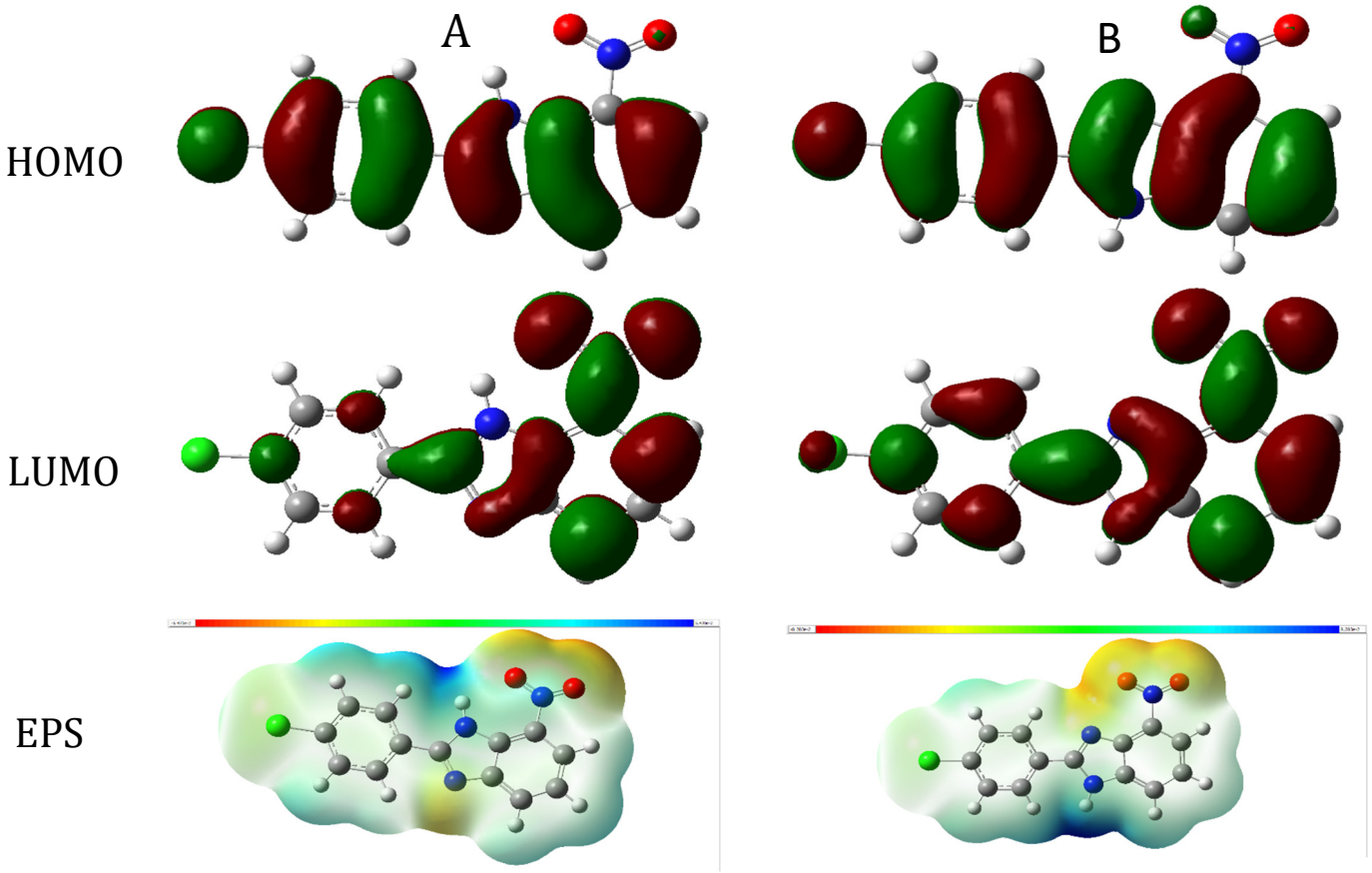


Figure 3. Distribution of the electronic densities and EPS of the HOMO and LUMO molecular orbitals calculated at the B3LYP/6-31G (d,p) level, for (**A**,**B**).

The calculated chemical parameters of our inhibitors are grouped in the following Table 1:

Table 1. Calculated quantum parameters for 2-(4-chlorophenyl)-4-nitro-1H-benzimidazole noted OS1 A and B.

Inhibitor	E_{HOMO} (eV)	E_{LUMO} (eV)	ΔE (eV)	χ (eV)	η (eV)	ΔN	E_{tot} (Hartrees)
A	−6.601	−2.895	3.706	4.748	1.853	0.019	−1273.789
B	−6.586	−2.602	3.984	4.594	1.992	0.057	−1274.207

3.2. Analysis of Quantum Parameters

The total energy of B tautomer is lower than the total energy of A (E_{tot}(B) > E_{tot}(A)), which implies that B is more stable than A.

The value ΔN = 0.019 for A and 0.057 is positive and less than 3.6, indicating that the molecule functions as an electron donor towards the iron substrate, creating a shielding layer that prevents corrosion.

We studied the local polarity of the OS1 on the two tautomer forms to identify potential electrostatic interactions with the external environment [15]. An ESP (electrostatic potential) analysis of the OS1 molecules was performed. This analysis is crucial for determining the active sites that will facilitate the adsorption of the corrosion inhibitor molecules onto the metal surface [16].

As illustrated in Figure 3, the electrostatic potential (ESP) gradually increases from red (electron-rich/negative) to blue (electron-poor/positive). The concentration of negative surface potential around the Nitrogen atom and two oxygens in OS1 demonstrates the

molecule's significant polarity. This suggests that the benzimidazole ring, containing these electron-rich C-N=C atoms, represents the primary site for electrostatic interactions with the external environment or the metal surface [17]. The electron-poor sites are localized in the nitrogen atoms (N-H) of the two forms of this compound. To confirm these results, we utilized Fukui functions, which are the most accurate.

Table 2, show the variation in Fukui indices for the two forms A and B of OBS14, Figure 1 indicate that C(4,6,24) N(12) O(15) and Cl(27) in A and C(4,5,6,32) O(14,15) and Cl(26) in B are the must nucleophilic sites and the must electrophilically sites are C(6) N(12) and O(15) in A and O(14,15) in B.

Table 2. Variation in Fukui indices as a function of two tautomer forms, A and B.

A			B		
Atoms	**f−**	**f+**	**Atoms**	**f−**	**f+**
1C	−0.016566	−0.047374	**1C**	−0.013019	−0.045176
2C	−0.018106	−0.04059	**2C**	−0.021956	−0.042397
3C	−0.036135	−0.03042	**3C**	−0.024001	−0.021362
4C	−0.047028	−0.047856	**4C**	−0.052389	−0.070314
5C	−0.045858	−0.076558	**5C**	−0.043725	−0.046155
6C	−0.066956	−0.029006	**6C**	−0.090607	−0.038453
7C	−0.050868	−0.037689	**7C**	−0.050387	−0.038067
11N	−0.052363	−0.008131	**11N**	−0.05106	−0.008412
12N	−0.025683	−0.055266	**12N**	−0.154575	−0.019192
13N	−0.02509	−0.021805	**13N**	−0.00935	−0.057787
14O	−0.082731	−0.02534	**14O**	−0.063185	−0.024072
15O	−0.092018	−0.041079	**15O**	−0.111207	−0.041922
16C	−0.022309	−0.037688	**17C**	−0.022417	−0.039755
17C	−0.02868	−0.036406	**18C**	−0.009521	−0.035894
18C	−0.034417	−0.034965	**19C**	−0.053163	−0.037644
19C	−0.030276	−0.031903	**20C**	−0.025297	−0.039215
21C	−0.028797	−0.039385	**22C**	−0.033482	−0.033433
23C	−0.04662	−0.052488	**24C**	−0.046318	−0.05382
26Cl	−0.07361	−0.122931	**27Cl**	−0.072962	−0.125952

4. Conclusions

In this work, we highlight the importance of the inhibitory activity of OS1 in these two tautomer forms, A and B. The DFT study facilitates the prediction of electrochemical activity and the identification of electrophilic and nucleophilic attack sites using Fukui functions. The value ΔN = 0.019 for A and 0.057 is positive and less than 3.6, indicating that the molecule functions as an electron donor towards the iron substrate, creating a shielding layer that prevents corrosion. Electrochemical studies, therefore, allow us to confirm that OS1 acts as a mixed-type inhibitor.

A theoretical DFT study will allow us to evaluate the inhibitory interest of each product before conducting an electrochemical survey to save time and target only those products that give good results in the theoretical study.

Author Contributions: Conceptualization, O.S., M.E. and M.C.; methodology, S.L. and A.I.; software, H.E. and D.A.; validation, M.E. and M.C.; formal analysis, O.S. and H.E.; investigation, M.C.; resources, M.E. and A.I.; data curation, O.S. and S.L.; writing—original draft preparation, O.S., M.E. and H.E.; writing—review and editing, O.S., M.E. and H.E.; visualization, D.A., and M.C.; supervision, M.E. and M.C.; All authors have read and agreed to the published version of the manuscript.

Funding: This research received no external funding.

Institutional Review Board Statement: Not applicable.

Informed Consent Statement: Not applicable.

Data Availability Statement: All data supporting this study are provided in the Section 3 of this paper.

Acknowledgments: Support for this work by Sultan Moulay Slimane University is gratefully acknowledged.

Conflicts of Interest: The authors declare no conflicts of interest.

Abbreviations

The following abbreviations are used in this manuscript:

DFT	Density functional theory
OS1	2-(4-chlorophenyl)-4-nitro-1H-benzimidazole
CS	Carbon steel
VIH	Human Immunodeficiency Virus

References

1. Al-Amiery, A.A.; Isahak, W.N.R.W.; Al-Azzawi, W.K. Corrosion Inhibitors: Natural and Synthetic Organic Inhibitors. *Lubricants* **2023**, *11*, 174. [CrossRef]
2. Chen, C.; Jin, H.; Wang, P.; Sun, X.; Jaroniec, M.; Zheng, Y.; Qiao, S.Z. Local reaction environment in electrocatalysis. *Chem. Soc. Rev.* **2024**, *53*, 2022–2055. [CrossRef] [PubMed]
3. Laghlimi, C.; Moutcine, A.; Ziat, Y.; Belkhanchi, H.; Koufi, A.; Bouyassan, S. Hydrogen, Chronology and Electrochemical Production. *Sol. Energy Sustain. Dev. J.* **2024**, *14*, 22–37. [CrossRef]
4. Desai, P.D.; Pawar, C.B.; Avhad, M.S.; More, A.P. Corrosion inhibitors for carbon steel: A review. *Vietnam J. Chem.* **2023**, *61*, 15–42. [CrossRef]
5. Rakib, E.M.; Boga, C.; Calvaresi, M.; Chigr, M.; Franchi, P.; Gualandi, I.; Ihammi, A.; Lucarini, M.; Micheletti, G.; Spinelli, D.; et al. A multidisciplinary study of chemico-physical properties of different classes of 2-aryl-5(or 6)-nitrobenzimidazoles: NMR, electrochemical behavior, ESR, and DFT calculations. *Arab. J. Chem.* **2021**, *14*, 103179. [CrossRef]
6. Bai, S.; Zhang, M.; Tang, S.; Li, M. Research Progress on Benzimidazole Fungicides: A Review. *Molecules* **2024**, *29*, 1218. [CrossRef] [PubMed]
7. Ran, B.; Wei, Z.; Yu, S.; Zhi, H.; Yan, S.; Cai, S.; Wen, L.; Fan, B.; Wang, J.; Wang, K.; et al. The study on corrosion inhibition effect of 2-Phenylbenzimidazole for X70 steel in HCl solution at 308 K. *Int. J. Electrochem. Sci.* **2023**, *18*, 100032. [CrossRef]
8. Behjatmanesh-Ardakani, R.; Imanov, H.A. DFT study on the mechanism of benzimidazole synthesis from phenylenediamine and formic acid: Activation energies and transition states' locations. *Chem. Rev. Lett.* **2025**, *8*, 1188–1199. [CrossRef]
9. Zhu, Z.; Lippa, B.; Drach, J.C.; Townsend, L.B. Design, Synthesis, and Biological Evaluation of Tricyclic Nucleosides (Dimensional Probes) as Analogues of Certain Antiviral Polyhalogenated Benzimidazole Ribonucleosides. *J. Med. Chem.* **2000**, *43*, 2430–2437. [CrossRef] [PubMed]
10. Zouaghi, M.O.; Bensalah, D.; Hassen, S.; Arfaouia, Y.; Mansourc, L.; Özdemird, N.; Bülbüld, H.; Gurbuze, N.; Özdemire, I.; Hamdi, N. Benzimidazole derivatives as a new scaffold of anticancer agents: Synthesis, optical properties, crystal structure and DFT calculations. *Heliyon* **2024**, *10*, e32905. [CrossRef] [PubMed]
11. Ihammi, A.; Chigr, M.; Ketatni, E.M.; Saadi, M.; El Ammari, L.; Rakib, E.M. Synthesis of new α-amino-1H indazolyl-phosphonate derivatives: Crystal structure, Hirshfeld surface analysis and DFT studies. *J. Mol. Struct.* **2020**, *1220*, 128702. [CrossRef]
12. Lazanas, A.C.; Prodromidis, M.I. Electrochemical Impedance Spectroscopy—A Tutorial. *ACS Meas. Sci. Au* **2023**, *3*, 162–193. [CrossRef] [PubMed]
13. Kadhim, A.; Betti, N.; Al-Bahrani, H.A.; Al-Ghezi, M.K.S.; Gaaz, T.; Kadhum, A.H.; Alamiery, A. A mini review on corrosion, inhibitors and mechanism types of mild steel inhibition in an acidic environment. *Int. J. Corros. Scale Inhib.* **2021**, *10*, 861–884. [CrossRef]
14. Yang, B.; Lv, Y.; Zhang, Z.; He, X.; Zhu, Y. Anticorrosion mechanism of natural acidic amino acids on steel in chloride solution: Experimental, theoretical and machine learning approaches. *J. Build. Eng.* **2023**, *79*, 107801. [CrossRef]
15. Liu, Z.; Lu, T.; Chen, Q. Intermolecular interaction characteristics of the all-carboatomic ring, cyclo[18]carbon: Focusing on molecular adsorption and stacking. *Carbon* **2021**, *171*, 514–523. [CrossRef]

16. Nesane, T.; Madala, N.E.; Kabanda, M.M.; Murulana, L.C.; Bahadur, I. Lippia javanica leaf extract as an effective anti-corrosion agent against mild steel corrosion in 1 M HCl and its characterization by UHPLC/Q-TOF-MS spectroscopy and quantum chemical evaluation of its adsorption process on Fe(110). *Colloids Surf. A Physicochem. Eng. Asp.* **2023**, *667*, 131405. [CrossRef]
17. Xu, J.; Li, H.; Jin, Y.; Zhou, D.; Sun, B.; Armand, M.; Wang, G. Understanding the Electrical Mechanisms in Aqueous Zinc Metal Batteries: From Electrostatic Interactions to Electric Field Regulation. *Adv. Mater.* **2024**, *36*, 2309726. [CrossRef] [PubMed]

Disclaimer/Publisher's Note: The statements, opinions and data contained in all publications are solely those of the individual author(s) and contributor(s) and not of MDPI and/or the editor(s). MDPI and/or the editor(s) disclaim responsibility for any injury to people or property resulting from any ideas, methods, instructions or products referred to in the content.